




Performance estimation of photovoltaic energy production

Laura Casula¹ · Guglielmo D'Amico² · Giovanni Masala¹  · Filippo Petroni³

Received: 31 May 2020 / Accepted: 16 October 2020
© The Author(s) 2020

Abstract

This article deals with the production of energy through photovoltaic (PV) panels. The efficiency and quantity of energy produced by a PV panel depend on both deterministic factors, mainly related to the technical characteristics of the panels, and stochastic factors, essentially the amount of incident solar radiation and some climatic variables that modify the efficiency of solar panels such as temperature and wind speed. The main objective of this work is to estimate the energy production of a PV system with fixed technical characteristics through the modeling of the stochastic factors listed above. Besides, we estimate the economic profitability of the plant, net of taxation or subsidiary payment policies, considered taking into account the hourly spot price curve of electricity and its correlation with solar radiation, via vector autoregressive models. Our investigation ends with a Monte Carlo simulation of the models introduced. We also propose the pricing of some quanto options that allow hedging both the price risk and the volumetric risk.

Keywords Solar radiation · Climatic variables · Income · Monte Carlo simulation · Electricity price · Quanto option

JEL Classification C53 · G17 · Q47

✉ Giovanni Masala
gb.masala@unica.it

Laura Casula
laura.casula@gmail.com

Guglielmo D'Amico
g.damico@unich.it

Filippo Petroni
f.petroni@univpm.it

¹ Dipartimento di Scienze Economiche e Aziendali, Università degli Studi di Cagliari, 09123 Cagliari, Italy

² Dipartimento di Economia, Università G. D'Annunzio, 66013 Chieti, Italy

³ Dipartimento di Management, Università Politecnica delle Marche, 60121 Ancona, Italy

1 Introduction

The production of renewable energies, such as wind and photovoltaic (hereinafter PV) energy, has been undergoing a significant increase in recent years. The installation of wind turbines and PV panels is currently booming, and this trend is expected to continue in the near future. These systems allow injecting on the market (in addition to a possible personal use) electricity with low environmental impact and with relatively low production costs. The “green energy” thus produced has an important impact on electricity prices through the typical auction mechanism in the day-ahead market (Deane et al. 2017). PV panels exploit direct solar radiation and they produce energy through the well-known photoelectric effect mechanism. The efficiency and quantity of energy produced depend on both deterministic and stochastic factors. The deterministic factors are mainly related to the technical characteristics of the panels: physical characteristics of the semiconductor materials (such as silicon), inclination of the panel and the azimuth angle of the panel surface. The stochastic factors are the amount of incident solar radiation and the climatic variables: for example, temperature and wind speed influence the mechanism of energy production through the photoelectric effect. The first objective of this research is to estimate the energy production of a PV plant with known technical characteristics. In this regard, we will have to effectively model the stochastic variables that come into play, namely the solar radiation (the basic variable) and the two climatic variables, temperature, and wind speed, which will affect the efficiency of the panels. Moreover, we estimate the economic profitability of the PV plant taking into account the hourly spot price curve of electricity in the day-ahead market. In this way, we can estimate not only the quantity of energy produced in a fixed time horizon but also the corresponding market value. In this respect, it is important to build up a model that considers among its features the correlation (on an hourly basis) between solar radiation and the price of electricity. Note that to evaluate the net income in the production of renewable energy, a much-debated topic currently, we could consider the production costs for individual technologies. For example, a recent study presented by IRENA (2019), *Renewable Power Generation Costs in 2018*, estimates an average cost for the production of PV energy equal to 0.085 USD/kWh. For comparison, the average cost of wind power generation is USD 0.056/kWh. Regarding the influence of any taxation or incentives in the production of PV energy, we are not currently aware of these data. In any case, these are fixed and deterministic values that do not lead to any modification of the models used so far. Finally, the correct assessment of the energy produced by PV panels and of the corresponding electricity prices allows the management of two important sources of uncertainty: the volumetric risk and the price risk. The volumetric risk regards the fact that in a fixed time horizon the production is lower than that planned by the producer therefore he is not able to meet the expected commitments. The price risk concerns a decrease in electricity spot prices and the corresponding fall of the expected income. These two types of risk can overlap and therefore lead to even greater losses. We show how quanto options can contribute to the solution

to this problem. Results are illustrated through Monte Carlo simulation in relation to a hypothetical PV system located in Italy. The main references in the literature regarding the pricing of these options can be traced back to the works of Benth et al. (2015), Benth and Ibrahim (2017) and Caporin et al. (2012). Regarding the production of PV energy, some works use neural network techniques, for example, Graditi et al. (2016). Benth and Ibrahim (2017) use daily data of some PV plants located in Germany and determine a continuous-time process suitable to model the daily PV production. Finally, Lingohr and Müller (2019) determine a non-linear continuous-time autoregressive process for the production of solar energy by using infeed data in Germany. Neto et al. (2017) aim to perform a portfolio optimization of RES generation assets (hydroelectric, wind, and PV) for the Brazilian market. They also present an economic analysis by taking into account taxation and financing for the determination of the associated cash flows, but they do not take into account the spot electricity prices. The empirical analysis of the data has highlighted, through the correlation, the presence of a certain dependence structure between solar radiation and the price of electricity. Besides, solar radiation assumes minimum values at night (for obvious reasons) and maximum values in the central hours of the day (1–2 pm). At the same time, the price of electricity also takes on higher values in the central hours of the day due to greater electricity demand. Consequently, we have introduced this feature into our model. The principal innovative aspect of our work concerns the modeling of the stochastic factors that come into play and the analysis of the profitability of a PV system that takes into account the real price of electricity: we used a multivariate model that could link the price of electricity with solar radiation (and therefore PV production) through a vector autoregressive process. In this way, we can more effectively evaluate both the income of the PV plant and more accurately price the joint market/volumetric risk through the quanto options. Pricing these options through a multivariate model is another original feature of our contribution. The next sections are structured as follows. In Sect. 2 we describe the factors that influence PV production. In Sect. 3 we present the models relating to the stochastic factors necessary to estimate the production and profitability of PV energy. Then, in Sect. 4, we reveal the results of the model and we price the quanto options.

2 Materials and methods

2.1 Photovoltaic production

To determine the energy produced by a PV panel, we follow a procedure used by Urraca et al. (2018). The standard test conditions (“STC”) foresee a temperature equal to 25 °C and an irradiation level 1000 W/m². In general conditions, the energy instantly produced by a PV panel depends on the effective in-plane radiation G_{eff} and the module temperature T_{mod} . First, we must determine the module temperature through the Faïman relation (Faïman 2008):

$$T_{\text{mod}} = T_{\text{amb}} + \frac{G_{\text{eff}}}{u_0 + u_1 \cdot \text{WS}_{\text{mod}}} \quad (1)$$

The parameter u_0 represents the effect of the radiation on the module temperature and u_1 explains the cooling by the wind. This relation allows determining the module temperature as a function of radiation in the incidence plane G_{eff} , the ambient temperature T_{amb} and the wind speed WS_{mod} measured at the device height. The u_0 and u_1 coefficients have been estimated empirically for different types of PV panels. A discussion is given by Koehl et al. (2011) from which we took the values used in the numerical application. Finally, the energy produced in general conditions can be obtained from the relation (Benth and Benth 2011; Urraca et al. 2018):

$$P'_{\text{DC}} = G'_{\text{eff}} \cdot \left(1 + k_1 \cdot \ln G'_{\text{eff}} + k_2 \cdot \ln^2 G'_{\text{eff}} + k_3 \cdot T'_{\text{mod}} + k_4 \cdot T'_{\text{mod}} \cdot \ln G'_{\text{eff}} + k_5 \cdot T'_{\text{mod}} \cdot \ln^2 G'_{\text{eff}} + k_6 \cdot T'^2_{\text{mod}} \right)$$

$$\begin{aligned} P'_{\text{DC}} &= P_{\text{DC}}/P_{\text{STC}} & P_{\text{STC}} &= \text{nominal power} \\ \text{with } G'_{\text{eff}} &= G_{\text{eff}}/G_{\text{STC}} & G_{\text{STC}} &= 1000 \text{ W/m}^2 \\ T'_{\text{mod}} &= T_{\text{mod}} - T_{\text{STC}} & T_{\text{STC}} &= 25 \text{ }^\circ\text{C} \end{aligned}$$

so that P_{DC} is the energy actually produced. For the parameters k_1, \dots, k_6 we took the values used by Huld et al. (2011) for *c-Si* type panels. The effect of temperature on the performance of PV panels has been investigated by Barykina and Hammer (2017) so that it is necessary to include it to model the energy production. We assume, without loss of generality, that the panel is ground-mounted, i.e. at a typical height of about 2 m. For simplicity, we assume that our panel is oriented in such a way that the incident radiation is given by the global radiation inferred from the MERRA-2 dataset (object of our modeling).

2.2 Dataset characteristics

The hourly time series of climatic variables can be obtained from NASA's MERRA-2 project (<https://gmao.gsfc.nasa.gov/reanalysis/MERRA-2>). We have chosen an Italian location with coordinates long. 8.75 and lat. 39.5. This location corresponds to a Mediterranean-type climate (with good insolation all year round) and flat land that does not contain particular geographical obstacles to radiation. Next, we examine each variable in detail.

2.2.1 Solar radiation

The MERRA-2 code for solar radiation is SWGDN (surface_incoming_shortwave_flux). The data cover 40 years, from 1/1/1980 to 31/12/2019 on an hourly basis (see Table 1).

The zero values are reached before sunrise and after sunset. Besides, solar radiation has a maximum value for each geographical location and for each hour and day of the year which depends (in a "clear sky" condition) on the position of the sun. The actual value of the radiation at a given instant, therefore, represents

Table 1 Variables statistics—real values

Indicator	Solar radiation (W/m ²)	Temperature (°C)	Wind speed (m/s)	Electricity price (€/MWh)
Mean	205.96	17.42	2.81	66.0465
Std. Dev.	287.70	9.70	1.86	34.5806
Skewness	1.22	0.65	0.96	2.0632
Kurtosis	3.19	2.97	3.42	6.5268
Min.	0	-4.14	0.01	0
Max.	1030	49.68	12.47	450
N° obs.	350,640	140,256	140,256	138,072

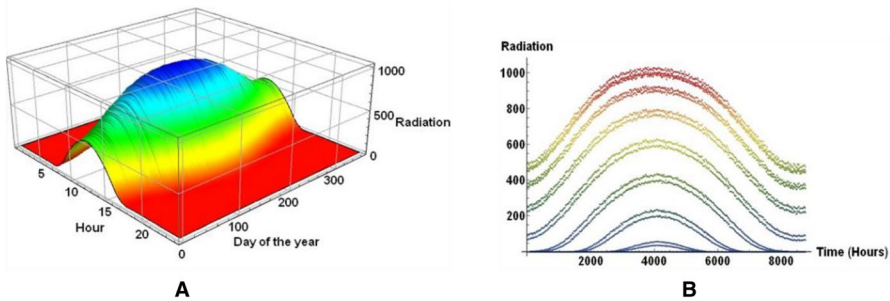


Fig. 1 (a) Maximum radiation vs. day/h. (b) Maximum radiation for each hour of the year

a fraction of the maximum radiation which depends on the atmospheric conditions (cloud cover, fog, presence of dust, etc. ...). The maximum radiation value can be estimated empirically by extracting the maximum radiation value for each hour and day of the year from the dataset (therefore each of these values will be estimated in a subset with 40 records). In Fig. 1a we report the maximum radiation as a function of the hour and day of the year (grid with 24×365 values) in a three-dimensional graph. In Fig. 1b we report the maximum radiation for the year (with an hourly period; 8760 values on the x -axis). The upper curve corresponds to hour 12 (with the upper value on 21 June), the lower curves correspond to hour 5 am and hour 7 pm.

Furthermore, we have noticed that the average radiation represents 82.55% of the corresponding maximum value therefore in this location the radiation reaches on average high values.

2.2.2 Temperature

The MERRA-2 code for temperature is TS. The data cover 16 years, from 1/1/2004 to 31/12/2019 on an hourly basis and 140,256 records (see Table 1 for

the main statistics). We note that extreme temperatures are unlikely. Temperatures that exceed 45 °C are only 0.33% while the negative ones are 0.66%.

2.2.3 Wind speed

The MERRA-2 codes for wind speed are U2M (*2-m eastward wind*) and V2M (*2-m northward wind*) which represent the two components. The wind speed is then deducted. The data cover 16 years, from 1/1/2004 to 31/12/2019 on an hourly basis (see Table 1). We observe that the wind speed remains rather low. Values higher than 10 m/s represent only 0.09% of the dataset. Let's assume that the PV panel is at a height of 2 m. Otherwise, we can exploit a well-known relationship (D'Amico et al. 2015b) to transform the intensity of the wind based on height. We also note that the average wind intensity depends on the hour: the average speed increases until it reaches a peak around hour 2 pm, then reverses the trend and decreases. Another aspect of the seasonality of the wind intensity can be deduced from the monthly average values. Finally, we examine the serial correlation for the series. For this purpose, we analyze the autocorrelation function (ACF) and partial correlation function (PACF) given in Fig. 5, Sect. 3.3. From these plots, we find evidence of the presence of serial autocorrelation at lags 1 and 2, while the series also denotes a clear seasonality of 24 h.

2.2.4 Electricity price

The data concerning electricity price is available from the Italian company “Gestore Mercati Energetici” website (<http://www.mercatoelettrico.org/It/download/DatiStorici.aspx>). We considered the Sardinia zonal price from 1/4/2004 to 31/12/2019 on an hourly basis since our PV plant is located in Sardinia (see Table 1). We note that prices exhibit a high kurtosis, due to the sudden peaks that characterize the electricity prices. Indeed, we note that although the average value is equal to 66.05 €/MWh, about 1% of the prices reach or exceed a threshold of 200 €/MWh. The price of electricity depends heavily on the hour and on the month, for example, from the

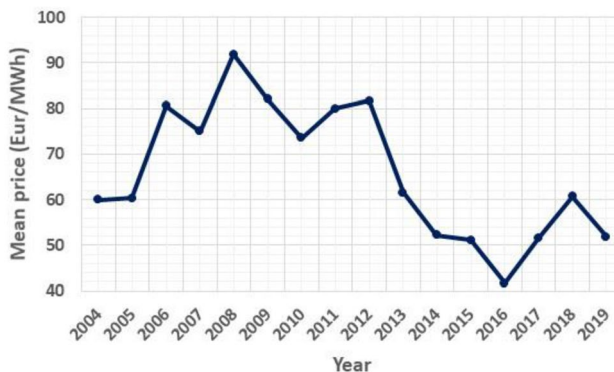


Fig. 2 Mean electricity price vs. year

dataset inspection, we highlight two maximum peaks at hours 10 am and 8 pm and the lowest values are found at night (for which the demand for energy drops). Average prices reach the lowest values between March and May, while higher values occur between July and September. The average price of electricity varies from year to year (see Fig. 2). In the reference period, the highest average price occurred in 2008 and the lowest in 2016.

3 Model

We advance a stochastic model for the main variables that come into play in Faiman's relation (1). We first propose autoregressive models of univariate time series of solar radiation, temperature, wind speed, and electricity prices and then we advance a more general scheme where solar radiation and electricity prices are modeled jointly in the form of a bivariate model. The application of Faiman's relation (1) to the results of the specific considered models allows quantifying the expected production and income.

3.1 The solar radiation

In Sect. 2.2.1 we determined an estimate of the maximum radiation for each hour of the day and each day. Now, the effective radiation $R(t)$ will be a stochastic fraction of the maximum radiation $R_{\max}(t)$ which depends on atmospheric factors.

We determine for each hour ($t=1, \dots, 8760$) and each year of the dataset, the fraction:

$$K(t) = \frac{R_{\max}(t) - R(t)}{R_{\max}(t)} \in [0, 1]$$

This fraction is defined when $R_{\max}(t) \neq 0$. Consequently, we deduce that $R(t) = R_{\max}(t) \cdot (1 - K(t))$. We note that a similar index denoted 'clearness index' was introduced by Koudouris et al. (2018). It represents the ratio between the effective solar radiation and the one measured at the top of the atmosphere. The authors model hourly clearness index for each month (for a total of 288 distributions) with a mixture of Kumaraswamy distributions. This method is particularly onerous in terms of parameters, so we prefer to model the variable $K(t)$ as a single process. To model the solar radiation, we just have to model the stochastic process $K(t)$ using the following process with white noise ε_1 :

$$K(t) = c_1 + A_1 \cdot \sin\left(\frac{2\pi}{24} \cdot t + B_1\right) + A_2 \cdot \sin\left(\frac{2\pi}{8760} \cdot t + B_2\right) + \sum_{i=1}^2 \alpha_i \cdot K(t-i) + \varepsilon_1$$

The seasonal component has two main periods (1 year and 24 h) that can be deduced from the single-sided amplitude spectrum (or the periodogram), besides the 24 h period can also be deduced from the ACF function (Fig. 3, top panel). Note

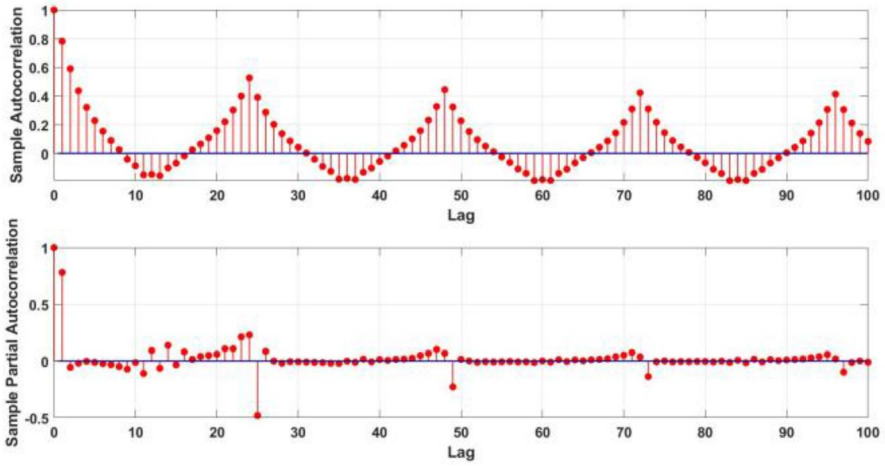


Fig. 3 ACF (top panel) and PACF (bottom panel) for $K(t)$ process

Table 2 Variables statistics—simulated values

Indicator	Solar radiation (W/m^2)	Temperature ($^{\circ}C$)	Wind speed (m/s)
Mean	210.03	17.43	2.81
Std. Dev.	279.25	9.69	1.78
Skewness	1.09	0.00	0.99
Kurtosis	2.89	2.42	4.24
Min.	0	-13.13	0.00
Max.	999.1	47.95	15.36
N° obs.	350,640	140,256	140,256

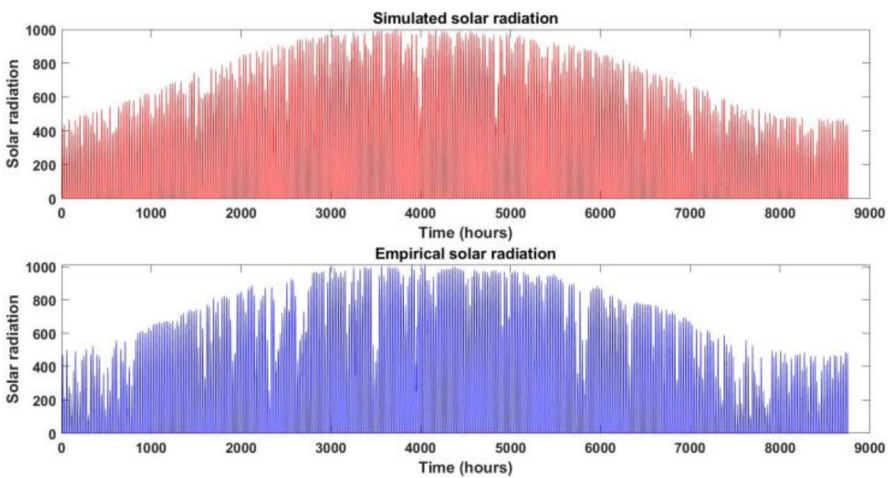


Fig. 4 Simulated and empirical solar radiation series (W/m^2)

that if we consider a single year dataset, the 1-year period is deleted. Next, we add an autoregressive component with two lags. To this end, we can examine the PACF function (Fig. 3, bottom panel).

The statistics of the simulated series are shown in Table 2 and are similar to the empirical values in Table 1.

Furthermore, we compare a simulated series in Fig. 4 (upper panel) with the empirical series (lower panel, referring to the last year of the dataset, where the x -axis comprises 8760 hourly values). We can see an excellent analogy of the data. This particular trajectory possesses the same qualitative characteristics as the empirical one. For example, zero values (corresponding to night hours) are positioned in the right place while the highest values are positioned around the summer solstice. Besides, the comparison between Tables 1 and 2 gives more reliable goodness of fit since this comparison was made with a certain number of simulated trajectories. For example, the difference in mean value is -1.98% and the difference in standard deviation is 2.94% , which are very low differences.

Neto et al. (2017) applied a mean-reverting model with a deterministic seasonality index to model directly the solar radiation. Here, we preferred to apply an autoregressive component to the $K(t)$ process since the maximum radiation is easily deduced from the empirical data.

3.2 Temperature

We can refer to the contributions of Benth and Benth (2011), Huang et al. (2018), Türkvtan et al. (2020) and Zapranis and Alexandridis (2011). The models described therein are aimed at pricing temperature-based derivatives and contain the main characteristics of temperatures series, namely, seasonality, autoregressive properties, and mean-reverting character. In accordance with the works listed, we decide to model the temperature using its known peculiarities, that is, a seasonal deterministic component and an autoregressive stochastic component. Let $T(t)$ be the temperature series on an hourly basis. The seasonal component is a combination of sinusoidal functions (with 1 year and 24 h main periods). Next, we model the residuals $\hat{T}(t)$ with an ARMA model. The optimal lags have been chosen with AIC and BIC criteria, we selected then an AR(3) process. We report the values of the estimated parameters in Table 3. The final process is (with white noise ε_2):

Table 3 Parameters of the ARMA component

	Value	p value
AR(1)	1.7927	0
AR(2)	-1.0739	0
AR(3)	0.2053	0

$$T(t) = c_2 + C_1 \cdot \sin\left(\frac{2\pi}{24} \cdot t + D_1\right) + C_2 \cdot \sin\left(\frac{2\pi}{8760} \cdot t + D_2\right) + \sum_{i=1}^3 \beta_i \cdot T(t-i) + \varepsilon_2$$

Next, we determine simulated trajectories from the model (see Table 2). A comparison with Table 1 (empirical data) shows a good fitting of the model. Indeed, the difference in mean value is -0.06% and the difference in standard deviation is 0.10% , which are very close values.

3.3 The wind speed process

Some models for wind speed have been developed by Caporin and Preš (2012), D'Amico et al. (2015a), Sim et al. (2019) and Casula et al. (2020). We have adopted the latter which allows being integrated into a bivariate model with the price of electricity. Let $W(t)$ be the wind speed at the time t . We apply at first the Box-Cox transformation given by the function (see e.g. Casula et al. 2020) $f_{\xi}(x) = \frac{x^{\xi}-1}{\xi}$. The transformed variable $\hat{W}(t) = f_{\xi}(W(t))$ has a distribution close to the Gaussian one. Next, we use a process similar to that used for temperature with white noise ε_3 :

$$\hat{W}(t) = c_3 + E_1 \cdot \sin\left(\frac{2\pi}{24} \cdot t + F_1\right) + E_2 \cdot \sin\left(\frac{2\pi}{8760} \cdot t + F_2\right) + \sum_{i=1}^2 \delta_i \cdot \hat{W}(t-i) + \varepsilon_3$$

The seasonal component has two main periods (1 year and 24 h) that can be deduced from the single-sided amplitude spectrum (if we consider a single year dataset, the 1-year period is deleted). Next, we add an autoregressive component with two lags. To this end, we can examine the ACF and the PACF function (Fig. 5, top/bottom panel respectively).

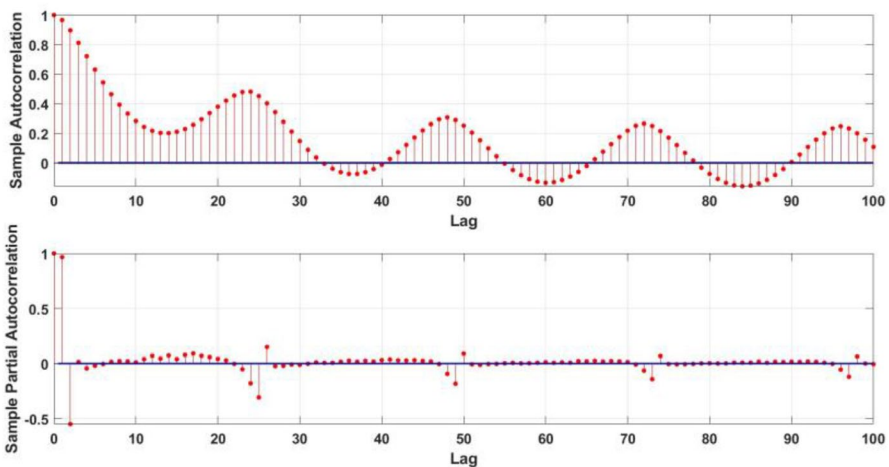


Fig. 5 ACF (top panel) and PACF (bottom panel) for wind speed process

The final step is to apply the inverse Box-Cox transformation $f_{\xi}^{-1}(x) = (1 + \xi \cdot x)^{1/\xi}$. The parameters of the model have been estimated through log-likelihood maximization (performed with Matlab tools, values omitted). Then, we simulate trajectories from this process through the Monte Carlo procedure. The statistics of the simulated series are reported in Table 2. A comparison with Table 1 (empirical data) shows a good fitting of the model. The difference in mean value is 0.00% and the difference in standard deviation is 4.30%, which are again very low differences.

3.4 The electricity price process

An overview of recent models was provided by Weron (2014) and Nowotarski and Weron (2018) and the bibliography included therein. We will use the approach developed in Casula et al. (2020) again in this context. Let $P(t)$ be the electricity price at the time t . The price process $P(t)$ has a non-Gaussian probability distribution (confirmed by the J-B test, see Casula et al. 2020) and is characterized by price peaks and near-zero values. To transform this distribution to a Gaussian one, we apply the $N-PIT$ transformation defined as (Nowotarski and Weron 2018; Uniejewski et al. 2019) $\tilde{P}(t) = G^{-1}(F_{P(t)}(P(t)))$ where $F_{P(t)}$ is the cumulative distribution function (CDF) of $P(t)$ and $\tilde{P}(t)$ is the transformed variable. As the real distribution of $P(t)$ is not known, we can estimate it with the empirical distribution function. Finally, G^{-1} is the inverse of the standard normal CDF. Next, we use a process similar to that used before, with white noise ε_4 :

$$\tilde{P}(t) = c_4 + M_1 \cdot \sin\left(\frac{2\pi}{24} \cdot t + N_1\right) + M_2 \cdot \sin\left(\frac{2\pi}{168} \cdot t + N_2\right) + M_3 \cdot \sin\left(\frac{2\pi}{8760} \cdot t + N_3\right) + \sum_{i=1}^2 \gamma_i \cdot \tilde{P}(t-i) + \varepsilon_4$$

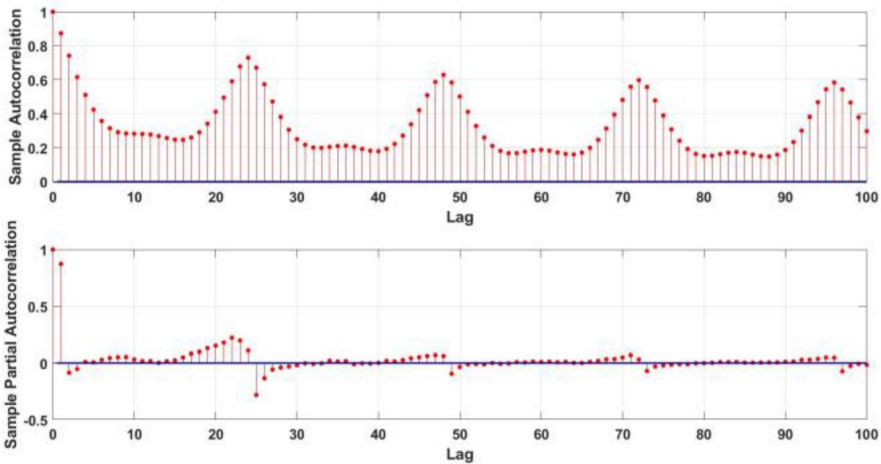


Fig. 6 ACF (top panel) and PACF (bottom panel) for electricity price process

Table 4 Simulated and empirical electricity price series statistics for the year 2019

Indicator	Empirical	Simulated
Mean	51.80	51.96
Std. Dev.	13.37	13.11
Skewness	-0.46	-0.41
Kurtosis	4.83	4.69
Min.	0	0
Max.	113.07	109.57

The seasonal component has three main periods (1 year, 1 week, and 24 h) that can be deduced from the single-sided amplitude spectrum (if we consider a single year dataset, the 1-year period is deleted). Next, we add an autoregressive component with two lags. To this end, we can examine the ACF and the PACF function (Fig. 6, top and bottom panel respectively). Finally, we simulated trajectories from the process through Monte Carlo procedure and applied the inverse N -PIT transformation $P(t) = F_{P(t)}^{-1}(G(\hat{P}(t)))$.

The parameters of the model have been estimated through log-likelihood maximization (performed with Matlab tools, values omitted). Then, we simulate trajectories from this process (statistics are reported in Table 4 for year 2019). A comparison with empirical data shows a good fitting. The difference in mean value is -0.31% and the difference in standard deviation is 1.94% , which are very low differences, so that the simulated values represent faithfully the real ones.

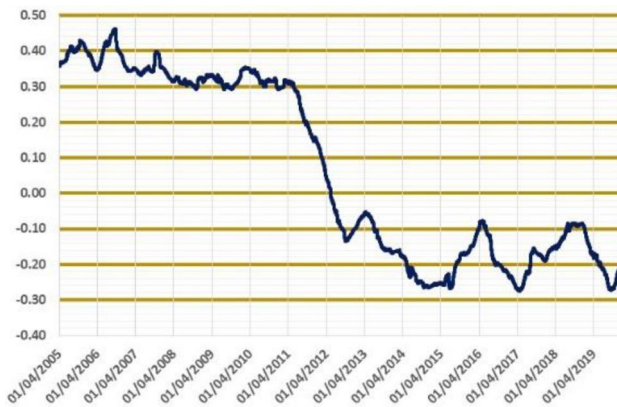
**Fig. 7** Correlation electricity price—solar radiation period 2005–2019

Table 5 Real correlations electricity price—solar radiation period 2009–2019

Year	2009	2010	2011	2012	2013	2014	2015	2016	2017	2018	2019
Corr.	0.3292	0.2932	0.1437	-0.0964	-0.1654	-0.2614	-0.1580	-0.2247	-0.1873	-0.0953	-0.1509

3.5 Electricity price: solar radiation bivariate model

We highlight that the correlation between the price of electricity and solar radiation has undergone considerable variations over time. In Fig. 7, we reported the correlation using a 1-year rolling window.

Finally, in Table 5 we list the correlations year by year. The salient fact concerns a sudden change in the period 2011–2012, indeed it is verified that the correlation passes from positive to negative values. Since the correlation changes considerably year by year, it is appropriate to create a bivariate model that can take this characteristic into account and to model these variables year by year separately.

To achieve this, in the models that describe the solar radiation and the price of electricity, we have replaced the respective AR(2) components with a single VAR (“vector autoregressive”) process. We used more specifically a VAR(2, 2) process with 2 variables and 2 lags. The bivariate model considered can therefore be written as follows:

$$\begin{cases} \hat{K}(t) = \sum_{i=1}^2 a_i \cdot \hat{K}(t-i) + \sum_{i=1}^2 b_i \cdot \hat{P}(t-i) + \eta_1 \\ \hat{P}(t) = \sum_{i=1}^2 m_i \cdot \hat{K}(t-i) + \sum_{i=1}^2 n_i \cdot \hat{P}(t-i) + \eta_2 \end{cases}$$

where η_1 and η_2 are white noises and $\hat{K}(t)$ and $\hat{P}(t)$ are the deseasonalized processes:

$$\begin{cases} \hat{K}(t) = K(t) - c_1 - A_1 \cdot \sin\left(\frac{2\pi}{24} \cdot t + B_1\right) \\ \hat{P}(t) = \tilde{P}(t) - c_4 - M_1 \cdot \sin\left(\frac{2\pi}{24} \cdot t + N_1\right) - M_2 \cdot \sin\left(\frac{2\pi}{168} \cdot t + N_2\right) \end{cases}$$

To explain the change in correlation in the period 2011–2012, we consider in Table 6 the quantity of energy from renewable sources produced in Italy and we note that since 2011 there has been a massive input of PV energy, which has exceeded wind power production (ISTAT source, <http://dati.istat.it/Index.aspx?lang=en&SubSessionId=cc36211b-d2d0-4c05-bb28-8d7c66cbd429>).

We can argue that an increase in PV production may lead to a decrease in prices due to the behavior of producers in the auction mechanism in the Day-Ahead Market.

3.6 The expected production and income

To determine the energy produced, we apply at first the Faiman relation (1). We use the values from Koehl et al. (2011): $u_0 = 26.9 \text{ W/}^\circ\text{C m}^2$; $u_1 = 6.20 \text{ Ws/}^\circ\text{C m}^3$. Precisely, we followed the choice of Huld and Gracia Amillo (2015), page 5163, which consists in taking the average value of the values reported by Koehl et al. (2011). Next, we apply the relation (2) from Urraca et al. (2018). The associated parameters are taken from Huld et al. (2011) for *c-Si* type panels: $k_1 = -0.017237$; $k_2 = -0.040465$; $k_3 = -0.004702$; $k_4 = 0.000149$; $k_5 = 0.000170$; $k_6 = 0.000005$.

Finally, we consider a nominal power $P_{\text{STC}} = 1 \text{ kW}$. Another important aspect of our work consists in determining the hypothetical profit deriving from the production of electricity in a fixed time horizon. To do this, we will use the zonal electricity price introduced earlier. The expected income at a time $t_0 \geq 0$ up to time $t_0 + \tau$ is:

$$V(t_0, t_0 + \tau) = \mathbb{E}_{t_0} \left[\sum_{k=1}^{\tau} P(t_0 + k) \cdot z(t_0 + k) \cdot (1 + r)^{-k} \right]$$

where r is a constant risk-free interest rate, $P(t_0 + k)$ is the price at the time $t_0 + k$ and $z(t_0 + k)$ is the energy produced at the time $t_0 + k$. An estimator of the expected income is:

$$\hat{V}(t_0, t_0 + \tau) = \frac{1}{H} \sum_{i=1}^H \sum_{k=1}^{\tau} P_i(t_0 + k) \cdot z_i(t_0 + k) \cdot (1 + r)^{-k} \quad (2)$$

where H is the number of simulations, $P_i(t_0 + k)$ is the value of the price process at the time $t_0 + k$ for the i th simulated path and $z_i(t_0 + k)$ has analogous meaning for the power production process. The estimation of the income through formula (2) considers the influence of the specific processes modeling the different variables as well as their interdependencies.

4 Results

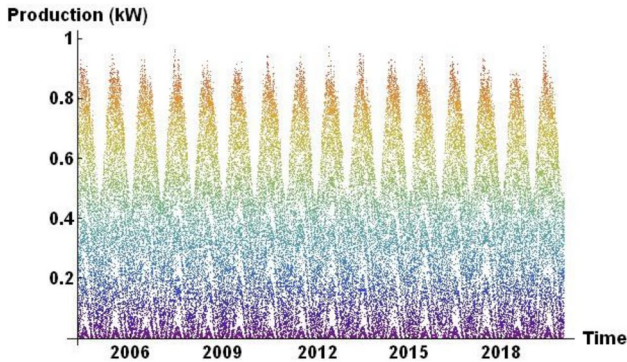
We first present the results about energy produced, then we generate implied incomes, and finally, quanto options are built for hedging risks. A comparison with the empirical values confirms the suitability of the proposed approach.

Table 6 Gross production of PV electricity (millions of KWh)

Year	2008	2009	2010	2011	2012	2013	2014	2015	2016	2017
PV	193.0	676.5	1905.7	10,795.7	18,861.7	21,588.6	22,306.4	22,942.2	22,104.3	24,377.7

Table 7 Empirical energy produced statistics (expressed in kW)

Indicator	Value	Indicator	Value	Indicator	Value
Mean	0.1890	Skewness	1.1304	Min.	0
Std. Dev.	0.2613	Kurtosis	2.8855	Max.	0.9720

**Fig. 8** Empirical energy produced (on an hourly basis for the period 2004–2019)

4.1 Energy production

The statistics of the empirical energy produced are reported in Table 7. We consider the dataset from 1/4/2004 (availability of the electricity price series) until 31/12/2019 (138,072 records) and we picture a synthetic series in Fig. 8.

We complete the analysis with a Monte Carlo simulation for which we have generated $ns = 100$ trajectories for each stochastic variable (see Table 8) and we note a good correspondence with the empirical values reported in the same table. Indeed, the differences in mean value (reported year by year) are respectively: -0.32% , 0.91% , 0.96% , -1.53% and -0.21% . Consequently, the simulated production values faithfully follow the empirical ones.

4.2 Income estimation

The results of the associated income estimated at the beginning of the time horizon (for the years 2015 to 2019) with a risk-free interest rate of 1% are shown in Table 9. We note here again a good correspondence between empirical and simulated values. Indeed, the differences in mean value (reported year by year) are respectively: -0.38% , -3.00% , -2.03% , -2.07% and -0.82% . Hence, the applied multivariate model allows us to reproduce faithfully the income, which contains all the stochastic variables introduced previously. The results are compared with those obtained by simulating the two series independently and in this case, a

Table 8 Real vs. simulated production for years 2015–2019

Year	Real mean production	Simulated mean production
2015	0.1892	0.1898
2016	0.1876	0.1859
2017	0.1977	0.1958
2018	0.1761	0.1788
2019	0.1892	0.1896

Table 9 Real vs. simulated incomes and simulated correlations price-solar radiation years 2015/2019

Year	Real income	Simulated income	Simulated income (indep.)	Correlation
2015	79,722.0	80,027.8	80,283.8	−0.1755
2016	62,458.0	64,331.9	65,489.5	−0.1507
2017	82,430.8	82,900.8	84,102.9	−0.1357
2018	90,979.9	92,866.8	94,738.7	−0.0973
2019	81,946.4	82,618.3	84,135.3	−0.1435

worse result is highlighted. We also report the correlation between the simulated electricity price and solar radiation series which are close to the real ones given in Table 5. Therefore, another strong point of the model is highlighted, namely the ability to reproduce the observed dependence structure.

4.3 Quanto options

The payoff associated with lower than expected energy production and electricity price can be expressed as a double put option $C(K_1, K_2) = \max(K_1 - E; 0) \cdot \max(K_2 - p; 0)$ with $E = \frac{1}{n} \sum_{i=1}^n E_i$; $p = \frac{1}{n} \sum_{i=1}^n p_i$. The “energy index” E is defined as the average energy produced over a specified horizon $[\tau_1, \tau_2]$ where E_i is the energy produced at a time i . The same holds for the price index p , where p_i denotes the spot price at a time i . The period is measured in hours and the horizon is arbitrary. The index n will then represent the number of hours in the given horizon. Finally, the strike values K_1 and K_2 are fixed. Assume that the quanto option is exercised at the time τ_2 . Its arbitrage-free price Q_t at time $t \leq \tau_2$ is given by (Benth et al. 2015) $Q_t = e^{-r \cdot (\tau_2 - t)} \mathbb{E}(C(K_1, K_2))$. Here, $r > 0$ denotes the risk-free interest rate (which we assume constant, as before). Since in our application, price and production levels differ widely year by year, we consider the options when referring to a specific year, evaluated at a time $t = \tau_1$. Regarding the pricing of this type of option, we can follow two distinct procedures. Benth et al. (2015, 2018) derive, in their application, a closed formula deduced from the hypotheses made on the dynamics of the underlying. Instead, Caporin et al. (2012) propose pricing through the Monte Carlo simulation, which allows dealing with more general situations (in the absence of closed formulas) but the method proves more onerous regarding processing times. Monte Carlo simulation was also used in Benth

and Ibrahim (2017), but there the authors directly modeled the production of PV energy instead of the factors that influence it. In our example, we followed the Monte Carlo simulation. For example, we report in Fig. 9 the values of the quanto option for the years 2016 and 2018. We considered a variable strike for both variables (production level and electricity price) therefore the option value is presented as a three-dimensional figure with respect to the strike values set as independent variables.

From the comparison between these two cases, we note that the same strikes range for both options leads to different fair values of the options. Consequently, it is clear that the quanto options should ideally offer hedging for a specific horizon. We can also deduce from these plots that the value of the quanto option increases as the strike values increase. Indeed, if we increase the strike values (namely the “planned” price and production values), it is more likely that the real values are below these planned values. Therefore, the cost of hedging against price/volumetric risk will be higher. Furthermore, it is interesting to note that if only one of the two strikes take on a “high” value, the option value is lower. In this situation, the price/volumetric risk does not exist simultaneously therefore the balance of these two situations leads to the fair price of the quanto option.

5 Discussion

The growing diffusion of renewable energies requires the creation of models to estimate the production and profitability of energy. In this work, we specifically dealt with the production of energy by PV panels that exploit the photoelectric effect. If we consider a PV panel with certain fixed technical characteristics, the amount of energy produced essentially depends on the amount of incident solar radiation. The efficiency of the panel also depends, to a certain extent, on temperature and wind speed. To correctly model the energy produced, we must therefore effectively model these three stochastic variables. We have described the models used in the work and we have shown that they allow us to fully replicate the empirical values. Finally, to evaluate the income deriving from the production of electricity, it is appropriate to correctly model the series of electricity prices. For this purpose, we applied a bivariate model solar radiation/electricity price to cope with the correlation between these two variables. We also described the model used in the work, and we verified that the simulated values

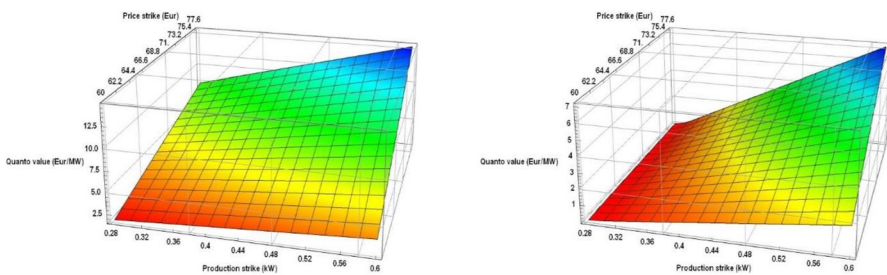


Fig. 9 Quanto option for the year 2016 (left panel) and the year 2018 (right panel)

also faithfully replicate the empirical values. More precisely, the comparison between empirical and simulated values takes place on different levels. First, we compared the individual variables (solar radiation, temperature, wind intensity, and electricity price). Subsequently, we compared the energy production and the income (where all 4 stochastic variables come into play). Besides, the VAR models used to estimate PV production and the price of electricity are sufficiently flexible and adapt to the description of data coming from sites with slightly different climatic conditions. The results of the estimates will give us slightly different parameters, but the general methodology remains unchanged. Moreover, the stochastic processes that represent the main climatic variables (solar radiation, wind intensity and temperature) are based on typical characteristics of these variables. Regarding the model of the electricity price, also in this case we have exploited the typical characteristics of this variable. The different zonal markets present in the Italian territory may present more or less high values but despite this, the qualitative characteristics are similar. A fundamental aspect of our model is to have considered the observed dependence structure between the price of electricity and solar radiation. This particularity is also valid outside the local context used for our numerical simulations so we can conjecture that the type of model used here can cover a wider field of application. Finally, taking into account that an energy producer is subject to both volumetric risk (lower than expected production) and price risk (drop in the spot price of electricity), we have developed quanto options useful to face these risks. These options were then priced with the Monte Carlo method.

Funding Open access funding provided by Università degli Studi di Cagliari within the CRUI-CARE Agreement.

Open Access This article is licensed under a Creative Commons Attribution 4.0 International License, which permits use, sharing, adaptation, distribution and reproduction in any medium or format, as long as you give appropriate credit to the original author(s) and the source, provide a link to the Creative Commons licence, and indicate if changes were made. The images or other third party material in this article are included in the article's Creative Commons licence, unless indicated otherwise in a credit line to the material. If material is not included in the article's Creative Commons licence and your intended use is not permitted by statutory regulation or exceeds the permitted use, you will need to obtain permission directly from the copyright holder. To view a copy of this licence, visit <http://creativecommons.org/licenses/by/4.0/>.

References

- Barykina, E., Hammer, A.: Modeling of photovoltaic module temperature using Faiman model: sensitivity analysis for different climates. *Sol. Energy*. **146**, 401–416 (2017)
- Benth, F.E., Benth, J.Š.: Weather derivatives and stochastic modelling of temperature. *Int. J. Stoch. Anal.* **2011**, 576791, 1–21 (2011). <https://doi.org/10.1155/2011/576791>
- Benth, F.E., Ibrahim, N.A.: Stochastic modeling of photovoltaic power generation and electricity prices. *J. Energy Markets*. **10**(3), 1–33 (2017). <https://doi.org/10.21314/JEM.2017.164>
- Benth, F.E., Lange, N., Myklebust, T.Å.: Pricing and hedging quanto options in energy markets. *J. Energy Markets*. **8**(1), 1–35 (2015)
- Benth, F.E., Di Persio, L., Lavagnini, S.: Stochastic modeling of wind derivatives in energy markets. *Risks*. **6**(2), 56 (2018). <https://doi.org/10.3390/risks6020056>
- Caporin, M., Preš, J.: Modeling and forecasting wind speed intensity for weather risk management. *Comput. Stat. Data Anal.* **56**, 3459–3476 (2012)

- Caporin, M., Preš, J., Torro, H.: Model based Monte Carlo pricing of energy and temperature Quanto options. *Energy Econ.* **34**, 1700–1712 (2012)
- Casula, L., D'Amico, G., Masala, G., Petroni, F.: Performance estimation of a wind farm with a dependence structure between electricity price and wind speed. *World Econ.* **43**, 2803–2822 (2020). <https://doi.org/10.1111/twec.12962>
- D'Amico, G., Petroni, F., Pratico, F.: Economic performance indicators of wind energy based on wind speed stochastic modeling. *Appl. Energy.* **154**, 290–297 (2015a)
- D'Amico, G., Petroni, F., Pratico, F.: Wind speed prediction for wind farm applications by Extreme Value Theory and Copulas. *J. Wind Eng. Ind. Aerodyn.* **145**, 229–236 (2015b). <https://doi.org/10.1016/j.jweia.2015.06.018>
- Deane, P., Collins S., Gallachóir, B.Ó., Eid, C., Hartel, R., Keles, D., Fichtner, W.: Impact on electricity markets: merit order effect of renewable energies. *Europe's Energy Transit Insights Policy Making* (Chapter 16) (2017). <https://doi.org/10.1016/B978-0-12-809806-6.00016-X>
- Faiman, D.: Assessing the outdoor operating temperature of photovoltaic modules. *Prog. Photovolt. Res. Appl.* **16**, 307–315 (2008). <https://doi.org/10.1002/pip.813>
- Graditi, G., Ferlito, S., Adinolfi, G.: Comparison of Photovoltaic plant power production prediction methods using a large measured dataset. *Renew. Energy.* **90**, 513–519 (2016)
- Huang, J.W., Yang, S.S., Chang, C.C.: Modeling temperature behaviors: application to weather derivative valuation. *J. Futur. Markets.* **38**, 1152–1175 (2018)
- Huld, T., Gracia Amillo, A.M.: Estimating PV module performance over large geographical regions: the role of irradiance, air temperature, wind speed and solar spectrum. *Energies.* **8**, 5159–5181 (2015). <https://doi.org/10.3390/en8065159>
- Huld, T., Friesen, G., Skoczek, A., Kenny, R.P., Sample, T., Field, M., Dunlop, E.D.: A power-rating model for crystalline silicon PV modules. *Sol. Energy Mater. Sol. Cells.* **95**, 3359–3369 (2011). <https://doi.org/10.1016/j.solmat.2011.07.026>
- IRENA: Renewable power generation costs in 2018. International Renewable Energy Agency, Abu Dhabi (2019). ISBN 978-92-9260-126-3.
- Koehl, M., Heck, M., Wiesmeier, S., Wirth, J.: Modeling of the nominal operating cell temperature based on outdoor weathering. *Sol. Energy Mater. Sol. Cells.* **95**, 1638–1646 (2011)
- Koudouris, G., Dimitriadis, P., Iliopoulou, T., Mamassis, N., Koutsyoiannis, D.: A stochastic model for the hourly solar radiation process for application in renewable resources management. *Adv. Geosci.* **45**, 139–145 (2018). <https://doi.org/10.5194/adgeo-45-139-2018>
- Lingohr, D., Müller, G.: Stochastic modeling of intraday photovoltaic power generation. *Energy Econ.* **81**, 175–186 (2019). <https://doi.org/10.1016/j.eneco.2019.03.007>
- Neto, D.P., Domingues, E.G., Coimbra, A.P., de Almeida, A.T., Alves, A.J., Calixto, W.P.: Portfolio optimization of renewable energy assets: hydro, wind, and photovoltaic energy in the regulated market in Brazil. *Energy Econ.* **64**, 238–250 (2017)
- Nowotarski, J., Weron, R.: Recent advances in electricity price forecasting: a review of probabilistic forecasting. *Renew. Sustain. Energy Rev.* **81**, 1548–1568 (2018)
- Sim, S.-K., Maass, P., Lind, P.G.: Wind speed modeling by nested ARIMA processes. *Energies.* **12**(1), 69 (2019). <https://doi.org/10.3390/en12010069>
- Türkvatan, A., Hayfavi, A., Omay, T.: A regime switching model for temperature modeling and applications to weather derivatives pricing. *Math. Finan. Econ.* **14**, 1–42 (2020)
- Uniejewski, B., Weron, R., Ziel, F.: Variance stabilizing transformations for electricity spot price forecasting. *IEEE Trans. Power Syst.* **33**(2), 2219–2229 (2019)
- Urraca, R., Huld, T., Lindfors, A.V., Riihelä, A., Martinez-de-Pison, F.J., Sanz-Garcia, A.: Quantifying the amplified bias of PV system simulations due to uncertainties in solar radiation estimates. *Sol. Energy.* **176**, 663–677 (2018)
- Weron, R.: Electricity price forecasting: a review of the state-of-the-art with a look into the future. *Int. J. Forecast.* **30**, 1030–1081 (2014)
- Zapranis, A.D., Alexandridis, A.: Modeling and forecasting cumulative average temperature and heating degree day indices for weather derivative pricing. *Neural Comput. Applic.* **20**, 787–801 (2011). <https://doi.org/10.1007/s00521-010-0494-1>